AN EXPERIMENTAL INVESTIGATION OF HEAT AND MASS TRANSFER IN A REACTING LAMINAR BOUNDARY LAYER ON A POROUS CYLINDER WITH PROPANE INJECTION

I. J. Kumar

UDC 536.244:532.517.2

This paper gives the results of an experimental investigation of heat and mass transfer in a reacting laminar boundary layer on a cylinder through which propane is injected for Re = $48 \cdot 10^4$–$4.6 \cdot 10^4$. Empirical equations are obtained for St and St_m. The effect of injection on the wall temperature and heat transfer is shown graphically.

Heat and mass transfer in the boundary layer on a porous wall in the presence of chemical reactions is widely used in modern technological processes. When the surface is protected from the very high temperature of the gas flowing over it by being made of a porous material through which a fuel coolant is injected, a boundary layer is formed on this surface. In many theoretical investigations, e.g., [1-3], attempts have been made to solve the problem by adopting various simplifying assumptions. There have been very few experimental investigations in this direction.

Kulgein [4] investigated complex processes of heat, mass, and momentum transfer in a turbulent boundary layer on a porous cylinder through which methane was injected. By considering the heat balance at the wall he derived a dimensionless criterion of heat and mass transfer in the chemically active boundary layer and showed that the dimensionless heat and mass transfer could be correlated by means of formulas of the form

$$St = 0.03\,Re_x^{-0.2}Pr^{-2/3}(T_w/T_\infty)^{0.4}, \quad (1)$$

$$St_m = 0.03\,Re_x^{-0.2}(Sc)^{-2/3}. \quad (2)$$

Smol'skii et al. [5, 6] investigated heat and mass transfer in a laminary boundary layer on a flat porous plate consisting of various sections through which alcohol and n hexane were injected with $(\rho v)_w$ = const; the injection rate varied in accordance with an $x^{-1/2}$ law.

This paper gives the results of an experimental investigation of heat and mass transfer in a laminar boundary layer on a porous cylinder with propane injection. In addition, the internal heat transfer in the porous wall is investigated theoretically and the results are compared with the experimental data.

The experimental cylindrical body, shown in section in Fig. 1, was mounted in a wind tunnel (Fig. 2) and consisted of a porous thin-walled cylinder 130 mm long, 3 mm wide, outer diameter 30 mm, pressed out of steel spheres, with a porosity P = 40%. The porous cylinder was cooled from inside by a soft copper coil 2, which almost touched its inside wall. A controlled flow of water passed through the coil so that it absorbed the heat released by the cooling porous wall and in this way the temperature of the fuel gas entering the tube was kept constant.

One end of the porous cylinder with the coil was rigidly attached to a cylindrical pillar 9 while the other was closed by a hemispherical copper cap with an orifice through which propane was admitted through tube 3. The cylindrical pillar also served as cladding for tubes 8 and 10, through which the cooling water entered, and for the leads of the thermocouples attached to the inside and outside surfaces of the porous cylinder. The porous cylinder was fitted with five alumel–chromel thermocouples (three on the outside and two on the inside) for measurement of the temperature along the cylinder and at different points on the

Delhi, India. Translated from Inzhenerno-Fizicheskii Zhurnal, Vol. 17, No. 4, pp. 622-632, October, 1969. Original article submitted December 13, 1968.

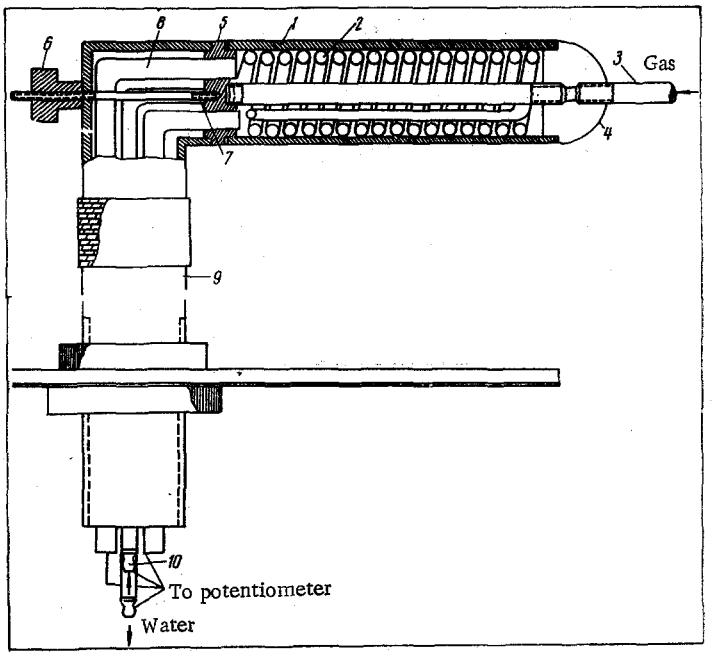

Fig. 1. General view of experimental body: 1) porous tube; 2) heat exchanger; 3) tube for admission of gas; 4) cap; 5) connecting sleeve; 6) nut; 7) connecting screw; 8, 10) tubes for cooling water and thermocouples; 9) cladding.

periphery of the cylinder. Thermocouples were also introduced into the inflowing and outflowing water for measurement of the temperature of the inflowing and outflowing water. The temperature of the fuel gas as it entered the porous wall was also measured with a thermocouple. The thermocouples were connected to an ÉPP automatic electronic potentiometer.

Using a VTI-2 chemical analyzer we determined the percentage CO, CO_2, O_2, and hydrocarbon content of gas samples taken at different distances from the porous wall. The local quenching effect was prevented by taking the gas samples through a stainless needle probe of diameter 0.5 mm connected to a tube of diameter 0.5 cm.

Before the experiment we switched on the wind tunnel and established a flow of the required velocity and temperature. The fuel gas was passed through the porous cylinder. The injection rate was regulated by a rotameter and the gas was ignited at the surface of the porous tube. We then passed water through the cooling coil and obtained a steady-state regime in which the temperatures on the inside and outside surfaces of the tube, the fuel gas at the entrance, and the inflowing and outflowing water were constant. The time required for establishment of the steady state was 5-8 min. On attainment of the steady state the thermocouple in the boundary layer, initially in contact with the surface of the porous body, was raised by steps of 20 μ to the plane of the reaction front and then by steps of 40 μ through the remaining thickness of the hot boundary layer.

From the experimental investigations we obtained the following data:

1) the rate of injection of fuel gas through the wall into the boundary layer;

2) the local temperatures and chemical composition of the gas over the thickness of the reacting boundary layer of the porous body;

3) the local temperature at different points on the inside and outside surfaces of the porous cylinder; the mean surface temperature was calculated from these results;

4) the temperature of the fuel gas as it entered the inside surface of the porous cylinder;

5) the flow rate of the water for cooling the porous surface, and the temperature of inflowing and outflowing water;

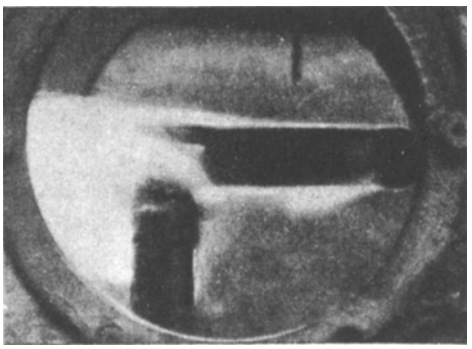

Fig. 2. General view of working chamber.

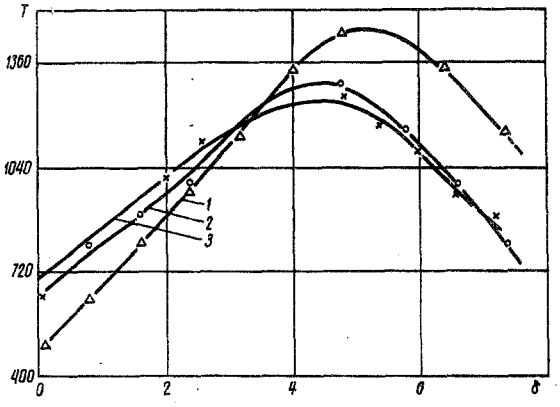

Fig. 3. Typical temperature profiles in boundary layer (T, °K; δ, mm): 1) F = 1.04 $\cdot 10^{-2}$; 2) $1.563 \cdot 10^{-3}$; 3) $1.062 \cdot 10^{-3}$.

6) the velocity and temperature of the air flow in the wind tunnel.

Figure 3 shows the temperature profiles in the boundary layer for Re = $0.642 \cdot 10^4$ and mainstream temperature 328°K. The graphs show that reduction of the wall temperature with increase in injection rate reduced the heat radiation from the wall to the surroundings, but the gradient on the wall was increased, which led to an increase in the amount of heat required to heat the injectant from the temperature at the entrance to the wall temperature. An increase in the injection rate moved the reaction front (front of maximum temperature) away from the porous wall. The resultant heat brought to the porous wall can be written as:

$$q_s = q_w - \varepsilon\alpha\left[\left(\frac{T_w}{100}\right)^4 - \left(\frac{T_\infty}{100}\right)^4\right]. \tag{3}$$

A rough estimate of q_S can be obtained from the temperature measurements inside and outside the porous plate, and also from calculations from the formula

$$\lambda_s(1-P)(T_{sw} - T_{sc})/\delta = q_s, \tag{4}$$

where λ_S is the thermal conductivity of solid steel, and T_{SC} is the temperature of the cooled wall surface. In this case P was assumed to be 40%. Thus, it is clear that we have at our disposal two independently obtained values of the heat flux, which can be used to calculate the Stanton number: from measurements of temperature in the main stream and on the hot surface and cooled surface of the porous wall. Although the temperature measurements in the boundary layer were usually made at the center of the cylinder, in some experiments measurements were made at three or four points along the porous wall so that we would have an idea of the variation of the coordinate of the reaction front along the tube. We found that the coordinate of the reaction front (maximum temperature) varied from 2 mm at a distance of L/4 from the start of the porous cylinder to approximately 4 mm at the end.

The cooling effect due to injection at the wall is illustrated by the data in Table 1, which relate to the wall temperature and correspond to a free-stream temperature of 300°K and different values of the injection parameter.

Hence, the wall temperature can be significantly reduced by injection of a chemically active coolant even at relatively low injection rates.

The problem of internal heat transfer in a porous plate through which a gas or liquid is transpired to cool the boundary layer has been solved by various authors. Some of them [7, 8] assumed that the temperature of the coolant inside the plate was equal to the temperature of the solid matrix, whereas others [9, 10] analyzed the problem on the assumption of a non-Newtonian type of transfer between the solid matrix and the coolant in the porous plate. In the present investigation we compared the experimental data for the resultant heat flux (total heat flux – radiation from surface) to the porous wall for the case of hot gases with the theoretical heat flux values obtained by solution of the problem of internal heat transfer with prescribed values of the cooling gas temperature, flow on the cooled wall side, and temperature of the solid matrix on the fuel gas side.

TABLE 1. Mean Temperature of Porous Wall in Relation to Injection Parameter

$F \cdot 10^3$	Mean wall temperature, °C	$F \cdot 10^3$	Mean wall temperature, °C
2,974	340	1,921	390
2,806	360	1,207	400
2,166	370	0,734	470

During the experiment we observed a large temperature difference over the thickness of the wall. The assumption of equality of the wall matrix and coolant temperatures in this case is incorrect. We can, however, obtain a solution consistent with all the experimental data by means of an analysis based on the assumption of the occurrence of non-Newtonian heat transfer between the solid body and coolant, if the heat flux and gas temperature on the coolant side are known. In some experimental works, e.g., [5], it was assumed that the wall obtains heat due to radiation from the hot gases. It was assumed in others [4] that the hot wall loses heat to the surrounding atmosphere. Thus, if the heat flux brought to the solid body is calculated by using the equations of internal heat transfer for a prescribed surface temperature (gas side of wall) and the results are compared with the experimental data for the heat fluxes from hot gases (obtained by calculation of the thermal conductivity involving the usual determination of the gas composition on the surface) the heat balance on the wall and the correctness of the Stanton number obtained above can be checked. Since the porous wall of the experimental cylindrical body was fairly thin, the temperature distribution in it could be calculated, as in the case of a thin plate, without significant error. On the assumption of inequality of the temperatures of the gas and solid body, Grootenhuis [9] deduced that the heat balance for an element dy at distance y from the entrance gives

$$\lambda_s \frac{d^2T_s}{dy^2} = h'(T_s - t_i) = J_m c_{pi} \frac{dt_i}{dy}. \tag{5}$$

Eliminating T, we obtain

$$\frac{d^3t}{dy^3} + \frac{h}{J_m c_{pi}} \frac{d^2t_i}{dy^2} - \frac{h}{\lambda_s} \frac{dt_i}{dy} = 0, \quad 0 \leqslant y \leqslant \delta, \tag{6}$$

where

$$t_i = T_s - \frac{1}{A} \frac{dt_i}{dy} \tag{7}$$

and

$$A = \frac{h}{J_m c_{pi}}. \tag{8}$$

We solve the upper equation with boundary conditions

$$y = 0 \quad \lambda_s \frac{dT_s}{dy} = \lambda_s \left(\frac{dt_i}{dy} + \frac{1}{A} \frac{d^2t_i}{dy^2} \right) = Q,$$
$$t_{ic} = T_s - \frac{1}{A} \frac{dT_s}{dy} = t_c; \tag{9}$$

$$y = \delta \quad T_s = t_i + \frac{1}{A} \frac{dt_i}{dy} = T_{sw}. \tag{10}$$

The solution of (5) with boundary conditions (9) and (10) can be written as:

$$T_s = t_c - \frac{QA}{h} + \left[\frac{Q}{\lambda_s} (\exp(-R\delta + S\delta) - \exp(S\delta - Ry)) + (R \exp(Sy) + S \exp(-Ry)) \left(T_{sw} - t_c + \frac{QA}{h} \right) \right] \Big/ C, \tag{11}$$

$$\lambda_s \left. \frac{dT_s}{dy} \right|_{y=\delta} = \left[h \left(T_{sw} - t_c + \frac{QA}{h} \right) (\exp(S\delta) - \exp(-R\delta)) + Q \exp(S\delta - R\delta) \right] / C, \tag{12}$$

where

TABLE 2. Experimental Data for Heat Flux Determination

No.	T_∞	T_w	T_{ic}	Q	Theoretical heat flux from (12)	Heat flux q_s^*
1	328	628	308	4,38	5,52	5,80
2	328	608	308	3,429	4,14	4,47
3	363	628	320	4,57	5,66	4,93
4	338	608	315	4,49	5,22	5,40
5	353	660	308	2,99	4,17	4,23
6	348	673	303	6,22	9,20	8,67
7	318	623	287	4,22	8,86	8,90
8	308	648	284	2,61	6,25	5,84
9	308	660	284	2,61	6,30	5,39
10	378	695	317	4,80	6,00	5,34
11	293	708	291	6,25	9,39	9,62
12	338	563	285	5,21	9,50	10,1

$$^{*}q_s = \left(\lambda_g \frac{\partial T_g}{\partial y}\right)_w - \alpha\varepsilon\left[\left(\frac{T_w}{100}\right)^4 - \left(\frac{T_\infty}{100}\right)^4\right].$$

$$R = B + A/2; \quad S = B - A/2; \quad B = \left[\frac{h}{\lambda_s} + \left(\frac{A}{2}\right)^2\right]^{1/2};$$

$$C = R\exp(S\delta) + S\exp(-R\delta).$$

Table 2 compares the values of the theoretical resultant heat flux on the gas side of the wall and the experimental values calculated from $q_S = q_W - \varepsilon\alpha[(T_W/100) - (T_\infty/100)^4]$. The value of h used in the above calculations was obtained from the graphs in [9].

It is easy to verify that the theoretical and experimental data agree to within ±10%.

Mass Transfer and Chemical Reactions. Typical profiles of temperature and C_3H_8, CO_2, and O_2 concentrations in the boundary layer are shown in Fig. 4 for $Re_x = 0.642 \cdot 10^4$ and $F = 2.868 \cdot 10^{-3}$. The concentration of the injectant at the surface equals 14.5%. The temperature profile shows that the maximum temperature front corresponds almost exactly with the chemical reaction front. The presence of water at any point on the boundary layer was determined by stoichiometric calculations for the percentage CO_2 composition at the corresponding point. The O_2 and CO_2 concentration profiles, as Fig. 4 shows, can easily be explained on the basis of theoretical data [3] for the case where the C_3H_8 injectant practically disappears in the reaction plane. The CO_2 and O_2 concentrations on the wall have finite values.

The fact that the reaction front is at a finite distance from the porous surface and not in direct contact with it shows that the chemical reaction does not proceed at an infinite rate and, hence, the diffusion and subsequent chemical reaction occur not in an infinitely thin zone, but in a zone of finite thickness. Hence, in the experimental investigations we do not encounter any temperature discontinuity and complete disappearance of the injectant at any point, as predicted theoretically on the basis of the hypothesis of an infinite reaction rate. The CO_2 component formed in the chemical reaction zone diffuses into the external medium and also to the porous wall. Since there is a very small amount of oxygen at the porous plate, CO_2 reacts with the gaseous injectant according to the reaction

$$C_3H_8 + 7CO_2 = 10CO + 4H_2O$$

and the CO obtained in this way diffuses to the reaction front.

The dimensionless heat and mass transfer coefficients in the boundary layer, viz., St and St_m, have the form

$$St = q_w/[\rho_\infty u_\infty (c_{pg})_\infty (T_* - T_w)], \tag{13}$$

$$St_m = \frac{M_\infty}{M_i}\frac{F(Sc)^{2/3}}{\ln(1-\chi)^{-1}} = \frac{29}{44}\frac{F(Sc)}{\ln(1-\chi)^{-1}}. \tag{14}$$

The resultant rate of heat transfer to the solid wall in equation (13) was calculated from the equation

$$q_s = \left(\lambda_g \frac{dT_g}{dy}\right)_w - \varepsilon\alpha\left[\left(\frac{T_w}{100}\right)^4 - \left(\frac{T_\infty}{100}\right)^4\right],$$

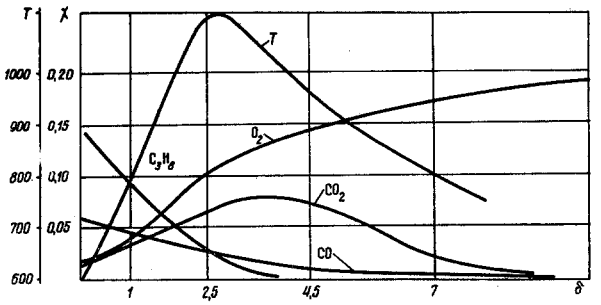

Fig. 4. Typical temperature and concentration profiles in boundary layer.

where $\alpha = 0.0014$ kcal $\cdot m^2 \cdot sec^{-1} \cdot deg^{-4}$ and $\varepsilon = 0.8$.

The thermal conductivity λ_g of the gas was calculated from the known composition of the gas on the wall and its temperature [11]; the temperature gradient was obtained from the measured temperature profile in the boundary layer.

Treatment of the experimental results by means of relationships of the form (1) did not lead to a satisfactory correlation of the results. In our case the experimental data were correlated by relationships of the form (1) to within ±30%. It is clear that none of the criteria mentioned above, viz., Re_x, Pr, or Sc, can satisfactorily describe the process in which the distinctive feature is a chemical reaction in the boundary layer. The large amount of heat released during the endothermic reactions in the boundary layer is responsible for the temperature profile, the wall temperature, and the temperature on the reaction front. In calculation of St the moving force of heat transfer is the flame temperature. Hence, it is desirable to find some other criteria for correlation of the experimental data. Considering the heat balance on the reaction front in the boundary layer we obtain the relationship

$$\left(\lambda \frac{\partial T}{\partial y}\right)_{II} - \left(\lambda \frac{\partial T}{\partial y}\right)_{I} = Q_R J_{u*}.$$

Assuming that the chemical reaction heat is transferred to the body by heat conduction we obtain

$$Q_R J_{u*} = \frac{\lambda_*}{l}(T_* - T_w),$$

where l is a characteristic length. We then obtain a new number

$$K = \frac{\lambda_w}{\lambda_*}\frac{T_* - T_w}{T_*} \quad \text{or} \quad K = \frac{\lambda_w}{\lambda_*}\frac{T_w}{T_*},$$

which was introduced before in [5, 6].

We found that the experimental values of St and St_m can be correlated to within ±17% by the formulas

$$St = 1.552\,Re_x^{-1/2}Pr^{-2/3}K^{1/4} \tag{15}$$

and

$$St_m = 0.648Re_x^{-\frac{1}{2}}(Sc)^{-2/3}K^{1/4}. \tag{16}$$

The experimental data and the results of correlation by these formulas are given in Fig. 5. The mean values of St without K are given in the form

$$St = 1.471Re_x^{-1/2}Pr^{-2/3}.$$

It should be noted that in the case of "pure" heat transfer the Stanton number can be expressed as

$$St = 0.332Re_x^{-1/2}Pr^{-2/3}.$$

The mean Stanton number corresponding to the formula given above can be written in the form

$$\overline{St} = 0.470Re_x^{-1/2}Pr^{-2/3}.$$

Thus, in our case heat transfer is much more intense than in the case of "pure" heat transfer. The reason for this intensity must be sought in the combined heat and mass transfer associated with the chemical

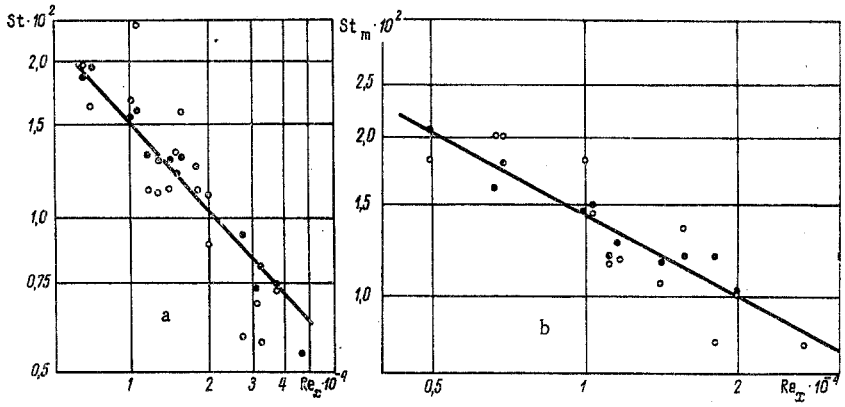

Fig. 5. St [from (15)] (a) and St_m [from (16)] (b) as functions of Re_x.

reaction, when heat transfer is increased by mass diffusion and the change in the physical properties of the gases. It was shown in an earlier paper [6] that the observed values of the Stanton numbers at constant injection rate are correlated by the formula

$$\overline{St} = 0.353 Re_x^{-1/2} Pr^{-2/3},$$

which shows that injection greatly reduces the heat transfer. The main difference between this investigation and [5, 6] lies in the fact that in the case of injectants like alcohol and hexane additional heat is spent on vapor formation. In addition, the resultant heat transfer q_s to the porous surface can be written as (neglecting radiation):

$$q_w = \left(\lambda_g \frac{\partial T_g}{\partial y}\right)_w - (\rho u)_w L.$$

In the case of a liquid injectant the presence of a second term on the right side of the equation greatly reduces the resultant rate of heat transfer to the wall and, hence, the Stanton number. As an analysis of the considered experimental data indicates, Sc varies from 0.91 to 1.12, and the corresponding Lewis number from 0.769 to 0.625. In addition, the value of Sc at flame temperature 1200°C is 2.08 times greater than the Prandtl number, and Le = 0.482. Thus, it is clear that we can hardly expect that the theoretical data of [2, 3], based on the simplifying assumptions of Pr and Sc equal to unity and constancy of thermophysical properties, characterize the considered process with satisfactory accuracy.

The author thanks Professor B. M. Smol'skii, Head of the Thermodynamics Laboratory of the Institute of Heat and Mass Transfer, Academy of Sciences of the Belorussian SSR, and also Candidate of Technical Sciences G. T. Sergeev and his colleagues, for help in conducting the experimental investigations described in the paper. The author also thanks the Director of the Laboratory (Delhi) for permission to publish this work.

NOTATION

St	is the heat transfer Stanton number;
St_m	is the mass transfer Stanton number;
$Re_x = u_\infty x/\nu$	is the Reynolds number;
$Pr = \nu/k$	is the Prandtl number;
$Sc = \nu/D$	is the Schmidt number;
$Le = D/k$	is the Lewis number;
ν	is the kinematic viscosity coefficient;
k	is the thermal diffusivity;
D	is the diffusion coefficient;
$F = (\rho v)_w/(\rho u)_\infty$	is the dimensionless injection parameter;
$J_m = (\rho v)_w$	is the injection rate;
u	is the velocity on x axis;
v	is the velocity on y axis;
x	is the coordinate in direction of flow;
y	is the coordinate perpendicular to main flow;

T	is the absolute temperature, °K;
λ	is the thermal conductivity;
$q_w = (\lambda_g dT_g/dy)_w$	is the total heat flux transferred to solid wall by hot gases on surface;
q_s	is the resultant heat flux to solid wall;
ε	is the wall emissivity;
α	is the emission coefficient;
ρ	is the density;
M	is the molecular weight;
h	is the heat transfer coefficient in porous body;
Q	is the mean heat flux from body to cooling wall, determined from amount of water passing through cooling tube and from difference in temperature of inflowing and outflowing water;
δ	is the thickness of porous wall;
c_p	is the specific heat;
χ	is the weight fraction of injectant at wall;
$K = (\lambda_g)_w/\lambda_*(T_g)_w/T_*$;	
L	is the latent heat of vaporization of injectant.

Subscripts

s	denotes the solid wall;
w	denotes the wall (on hot gas side);
c	denotes the wall (cooling wall);
*	denotes the flame front;
∞	denotes the main flow;
i	denotes the injectant;
g	denotes the main gas flow.

LITERATURE CITED

1. L. Lees, Jet Propulsion, 26, No. 4, 259 (1956).
2. E. R. G. Eckert and J. P. Hartnett, Proceedings of the Heat Transfer and Fluid Mechanics Institute, California (1958), p. 54.
3. C. B. Cohen, R. Bromberg, and R. P. Lipkis, Jet Propulsion, 28, 659 (1958).
4. N. G. Kulgein, J. Fluid Mech., 12, 417 (1962).
5. G. T. Sergeev and L. I. Tarasevich, in: Heat and Mass Transfer in Presence of Phase and Chemical Changes, Nauki i Tekhnika, Minsk (1968), p. 114.
6. G. T. Sergeev, B. M. Smol'skii, and L. I. Tarasevich, in: Heat and Mass Transfer in Presence of Phase and Chemical Changes, Nauka i Tekhnika, Minsk (1968), p. 126.
7. G. T. Sergeev, in: Heat and Mass Transfer in Capillary-Porous Solids, Nauka i Tekhnika, Minsk (1965), p. 74.
8. E. Mayer and J. G. Bartas, Jet Propulsion, No. 6 (1954).
9. P. Grootenhuis, J. Roy. Aeron. Soc., No. 578 (1959).
10. S. Weinhaum and H. L. Wheeler, J. Appl. Phys., 20, No. 1, 113 (1949).
11. S. Bretshnaider, Properties of Gases and Liquids [in Russian], Khimiya, Moscow – Leningrad (1966).